



# GAMOW-TELLER STRENGTH DISTRIBUTION IN THE $\beta$ -DECAY OF EXOTIC NUCLEI

J. Hardy, I. Towner

## ► To cite this version:

J. Hardy, I. Towner. GAMOW-TELLER STRENGTH DISTRIBUTION IN THE  $\beta$ -DECAY OF EXOTIC NUCLEI. Journal de Physique Colloques, 1984, 45 (C4), pp.C4-417-C4-431. 10.1051/jphyscol:1984432 . jpa-00224098

**HAL Id: jpa-00224098**

**<https://hal.science/jpa-00224098>**

Submitted on 4 Feb 2008

**HAL** is a multi-disciplinary open access archive for the deposit and dissemination of scientific research documents, whether they are published or not. The documents may come from teaching and research institutions in France or abroad, or from public or private research centers.

L'archive ouverte pluridisciplinaire **HAL**, est destinée au dépôt et à la diffusion de documents scientifiques de niveau recherche, publiés ou non, émanant des établissements d'enseignement et de recherche français ou étrangers, des laboratoires publics ou privés.

GAMOW-TELLER STRENGTH DISTRIBUTION IN THE  $\beta$ -DECAY OF EXOTIC NUCLEI

J.C. Hardy and I.S. Towner

*Atomic Energy of Canada Limited, Chalk River Nuclear Laboratories,  
Chalk River, Ontario, K0J 1J0, Canada*

**Résumé** - On décrit les résultats expérimentaux sur la distribution d'intensité Gamow-Teller obtenus à partir de la désintégration  $\beta$  de noyaux exotiques. Les résultats les plus complets, dans les noyaux légers, confirment l'absence d'intensité déjà notée dans les expériences (p,n). Dans les noyaux plus lourds, c'est la queue de la résonance qui est observée dans la désintégration  $\beta$ .

**Abstract** We describe experimental results on the Gamow-Teller strength distribution as obtained from the  $\beta$ -decay of exotic nuclei. The most complete results, in light nuclei, confirm the absence of strength noted in (p,n) measurements. In heavier nuclei it is the remote tail of the resonance that is established by  $\beta$ -decay.

## I - INTRODUCTION

Since  $\beta$ -decay strongly favours maximum energy release, it populates predominantly states at low excitation energy in the daughter nucleus. This has not prevented its study from contributing significantly to our understanding of nuclear structure but it is not often seen as meriting inclusion in a conference on highly excited states. The increased accessibility of nuclei far from stability is changing this perception. Today, it is commonplace to study the  $\beta$ -decay of a nucleus with  $Q\beta \gtrsim 10$  MeV, and experimental techniques are so sophisticated that good data are available on  $\beta$ -transitions or groups of transitions that are six orders of magnitude (or more) weaker than those populating states near the ground state. These transitions are indeed to highly excited states and, though weak, they can reflect important nuclear structure.

The decay rate,  $\lambda$ , for any allowed  $\beta$ -transition can be expressed in terms of the statistical rate function  $f$ , the Fermi and Gamow-Teller matrix elements,  $\langle 1 \rangle^2$  and  $\langle \sigma \rangle^2$  respectively, and the weak interaction coupling constants  $G_V$  and  $G_A$ :

$$\lambda = f[G_V^2 \langle 1 \rangle^2 + G_A^2 \langle \sigma \rangle^2]/K \quad (1)$$

where  $K = 1.775 \times 10^{-94} \text{ erg}^2 \text{ cm}^6 \text{ s}$ . The nuclear vector coupling constant is known from  $0^+ \rightarrow 0^+$   $\beta$ -decays [1] to be  $G_V = (1.4150 \pm 0.0003) \times 10^{-49} \text{ erg cm}^3$ , and the axial vector constant is known through the ratio  $G_A/G_V = 1.261 \pm 0.008$ , as obtained [2] from the decay of the neutron. Since the Fermi matrix element is only non-zero for (superallowed) transitions between analogue states, the ordinary allowed transitions, with which we shall be concerned here, can be described by:

$$\lambda = f \langle \sigma \rangle^2 (1.792 \pm 0.022) \times 10^{-4} \text{ s}^{-1} \quad (2)$$

For  $\beta$ -decay energies above a few MeV,  $f \approx E^5$ , which has the effect already noted of suppressing decays to excited states, even those with very favourable matrix elements.

The Gamow-Teller matrix element is given by

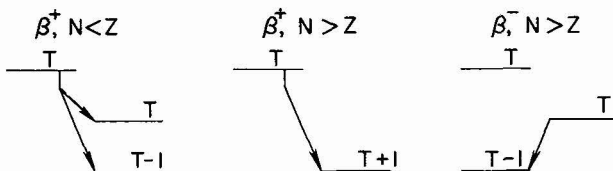
$$\langle \sigma \rangle = \langle \psi | \sum_n \sigma(n) \tau_{\pm}(n) | \psi \rangle_i \quad (3)$$

where  $\sigma$  is the Pauli spin operator and  $\tau_{\pm}$  the operator that converts a proton into a neutron, or vice versa. If nuclear forces were independent of spin, as they

nearly are of charge, then Gamow-Teller decay strength would be concentrated in the supermultiplet state, which in that case would coincide with the analogue state. In fact, because nuclear forces depend significantly on spin, those configurations that are populated by Gamow-Teller transitions are mixed over a wide energy region; nevertheless, as is by now well known, the transition strength is still collected in a "giant resonance" whose centroid corresponds to an excitation energy near, but slightly above, the analogue state /3/.

The energy of the Gamow-Teller giant resonance places profound limitations on our ability to observe its effects in nuclear  $\beta$ -decay. The decays of various classes of nuclei appear schematically in Fig. 1. Although only the lowest-energy states of each isospin are shown, it is evident that the Gamow-Teller resonance, being above the analogue state, is inaccessible in all cases except for the  $\beta^+$ -decay of  $N < Z$  nuclei. Even then, there are severe difficulties since only a portion of the

**Fig. 1** Schematic illustration of the  $\beta$ -decays of various classes of nuclei showing the lowest-energy states with the indicated isospin.



resonance may be energetically accessible, and at that, much of the accessible portion is populated by low energy - and consequently weak - transitions. In all other cases,  $\beta$ -decay explores only the remote tail of the giant resonance.

The most complete picture we have to date of the Gamow Teller resonance, as seen in  $\beta$ -decay is from data /4/ that are 12 years old. The  $T_Z = -3/2$  nucleus  $^{33}\text{Ar}$  has  $Q_\beta = 11.6$  MeV; because states populated above  $\approx 3$  MeV in its daughter,  $^{33}\text{Cl}$ , subsequently decay by proton emission, it has been possible to extract accurate  $\beta$ -decay branching ratios to states up to  $\approx 9$  MeV from the experimental spectrum of  $\beta$ -delayed protons. The corresponding values of  $\langle \sigma \rangle^2$  derived from equation (2), and combined in 250 keV bins, are illustrated in Fig. 2. The concentration of strength

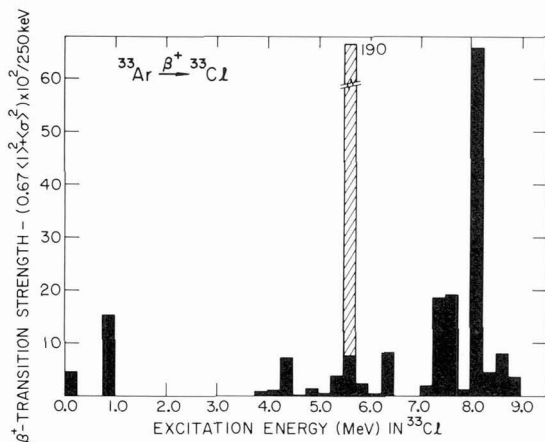


**Fig. 2** Distribution of transition strength for the  $\beta^+$ -decay scheme  $^{33}\text{Ar}(\beta^+)^{33}\text{Cl}$ . Decay to the analogue state is denoted by diagonal lines; solid bars correspond to Gamow-Teller strength.

at  $\approx 8$  MeV is suggestive of the Gamow-Teller resonance. It is worth noting, though, that the total  $\beta$ -decay branching to states above 6.0 MeV is 1.6%, to those below 1.0 MeV, 66%. The resonance region is certainly at the limits of observation.

In spite of these difficulties, does the bulk of the resonance really appear in Fig. 2? To answer, it will be necessary to compare the total observed  $\beta$ -decay

strength with some measure of the total strength available, and for this purpose it is convenient to introduce the sum rule /5/ already familiar in the study of Gamow-Teller resonances with charge-exchange reactions. If  $T_{\beta\pm}$  represents the total  $\langle\sigma\rangle^2$  observed in the  $\beta^\pm$ -decay of a given nucleus then:

$$\begin{aligned} T_{\beta-} - T_{\beta+} &= \sum_f \left[ \left| \langle \psi_f | \sigma_- | \psi_i \rangle \right|^2 - \sum_{f'} \left| \langle \psi_{f'} | \sigma_+ | \psi_i \rangle \right|^2 \right] \\ &= 3(N-Z) \end{aligned} \quad (4a)$$

In the study of (p,n) reactions, which are equivalent to  $\beta^-$ -decay, on stable nuclei with  $N > Z$ , this equation takes its usual form:

$$T_{\beta-} \geq 3(N-Z) \quad (4b)$$

However in light nuclei with  $Z > N$ , it is more useful as

$$T_{\beta+} \geq 3(Z-N) \quad (4c)$$

In both cases the equal sign more nearly applies if the complementary decay mode is inhibited by the unavailability of "spin-flip" states as a result either of a nearby closed shell or of a large neutron-proton imbalance, i.e. large values of  $|N-Z|$ .

In the case of  $^{33}\text{Ar}$  decay, equation (4c) becomes  $T_{\beta+} \geq 9$ . Since the integrated area of the histogram in Fig. 2 is 1.89, it seems unlikely that more than a portion of the resonance has been observed. Before drawing such a conclusion it is instructive to examine the distribution of Gamow-Teller strength distribution in a wider range of light nuclei.

## II - $\beta^+$ -DECAY OF LIGHT NUCLEI

As a result of the Coulomb energy,  $\beta^+$ -decay of a neutron-deficient nucleus releases more energy than the  $\beta^-$ -decay of the analogous (i.e. same value of  $|N-Z|$ ) proton-deficient nucleus. Thus, in principle, it is to  $\beta^+$ -decay that we must turn for the most complete view of the Gamow-Teller strength distribution. As a rather simple beginning, Fig. 3a illustrates the observed  $\beta^+$ -decay strength /6-8/ from the decay  $^{14}\text{O}(\beta^+)^{14}\text{N}$  as solid bars: only two states in  $^{14}\text{N}$  are seen to be populated within the 4 MeV energy range available to the decay. In addition, the  $\langle\sigma\rangle^2$  values derived /9/ from the mirror process,  $^{14}\text{C}(\text{p,n})^{14}\text{N}$ , are shown as the open bars for states energetically forbidden to  $\beta^+$ -decay. For comparison the results of three calculations with the Rochester-Oak Ridge shell-model code /10/ are shown in the same figure. The first (Fig. 3b), considered only p-shell configurations, with two-body matrix elements taken from ref. /11/. The other two (Fig. 3c,d) included the sd-shell through 2 particle-4 hole excitations in amounts determined by artificial adjustments to the particle-hole energy difference. Two-body matrix elements for the sd-shell were taken from ref. /12/.

It can be seen from Fig. 3 that the strength distribution broadens considerably with the amount of 2p-4h configuration mixing. At the same time, the total strength changes from  $T_{\beta+} = 6$  (the limiting value of equation 4c) for the p-shell calculation to  $T_{\beta+} = 7.1$  for the calculation of Fig. 3d. Despite the dramatic changes in distribution as the calculations change, the fraction of Gamow-Teller strength calculated within the 4 MeV " $\beta$ -decay window" remains remarkably constant at  $\approx 0.8$  as can be seen in Fig. 4. Also shown in the Fig. 4 is a comparable calculation for the decay  $^{18}\text{Ne}(\beta^+)^{18}\text{F}$ . Although the rate of change is greater in the latter case, spectrum considerations rule out large 2 particle-2 hole admixtures, with the result that the calculated fraction of  $T_{\beta+}$  within the window is again reasonably well determined.

If we believe that this fraction can be reliably calculated, then it is a simple matter to correct the observed Gamow-Teller strength, thus obtaining an estimate of the total strength. The results are shown in Table 1 for the cases already described. In addition, several other results are listed for the decay of T=1 nuclei. In these cases, calculations were less extensive, so no estimate of the uncertainty in the "calculated fraction" has been attempted.

Fig. 3

a) Experimentally determined values of  $\langle \sigma \rangle^2$  obtained from the decay  ${}^{14}\text{O}(\beta^+){}^{14}\text{N}$  (solid bars) and the reaction  ${}^{14}\text{C}(\text{p},\text{n}){}^{14}\text{N}$  (open bars).

b,c,d) Results of shell-model calculations described in text. The percentage configuration mixing refers to the ground state of the parent,  ${}^{14}\text{O}$ .

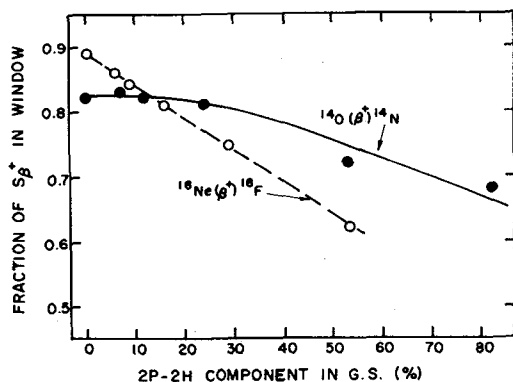
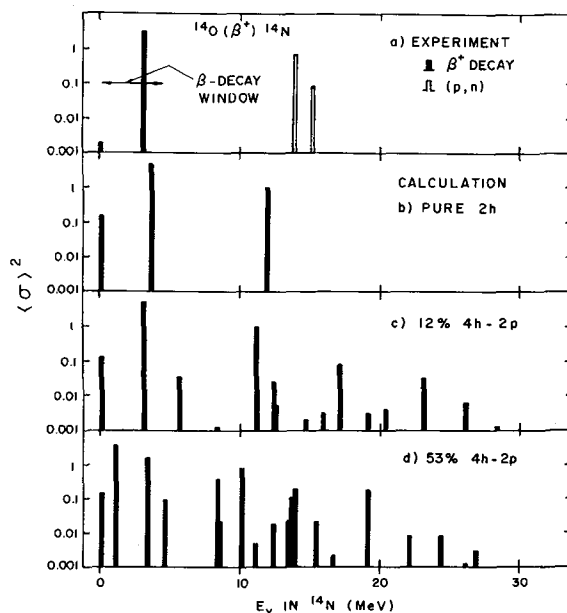


Fig. 4 Fraction of total Gamow-Teller strength  $T_{\beta^+}$  calculated to lie in the  $\beta$ -decay window for two decays, plotted as a function of the 2 particle-2 hole admixtures in the parent ground state.

Several observations can be made from the table. First, where the (p,n) reaction has been studied on the mirror nucleus, there is excellent agreement between the total strength so determined and that established from our approach. This is not too surprising since the (p,n) results are in fact "normalized" /9,14,15/ to one strong  $\beta^+$ -transition. Second, the four decays near closed shells show that  $T_{\beta^+} < 6$ , in violation of equation (4c). This supports the conclusion to this effect already noted from (p,n) measurements (eg. ref. /16/). For the two mid-shell cases, the shell-model calculations show considerable spreading of the strength, with only 10-30% lying within the  $\beta$ -decay window.

A complete survey of the Gamow-Teller strength observed in the decay of  $T_Z = -1$  nuclei is illustrated in Fig. 5. These results have not been corrected for unobserved transitions, as was done in Table 1. To first order, the transitions included within the heavy arrows should obey the limiting sum rule, i.e.  $T_{\beta^+} = 6$ ; all others should have  $T_{\beta^+} > 6$ . The fact that the latter actually show lower values of observed strength simply reflects the more complicated configurations,

Table 1: Experimentally observed Gamow-Teller strength

$\beta^+$ decay	Total $\langle\sigma\rangle_a^2$ observed	Calculated fraction in window	$T_{\beta^+}$	(p,n) Reaction	Equivalent $T_{\beta^+}$
$^{14}\text{O}(\beta^+)^{14}\text{N}$	$3.08 \pm 0.12$	$0.81 \pm 0.01$	$3.80 \pm 0.16$	$^{14}\text{C}(\text{p,n})^{14}\text{N}$	$3.87^b)$
$^{18}\text{Ne}(\beta^+)^{18}\text{F}$	$3.27 \pm 0.02$	$0.84 \pm 0.05$	$3.90 \pm 0.24$	$^{18}\text{O}(\text{p,n})^{18}\text{F}$	$3.97^c)$
$^{22}\text{Mg}(\beta^+)^{22}\text{Na}$	$2.28 \pm 0.06$	$\approx 0.30$	$\approx 8$		
$^{34}\text{Ar}(\beta^+)^{34}\text{Cl}$	$1.75 \pm 0.11$	$\approx 0.13$	$\approx 13$		
$^{38}\text{Ca}(\beta^+)^{38}\text{K}$	$1.93 \pm 0.11$	0.65	$2.98 \pm 0.35^d)$		
$^{42}\text{Ti}(\beta^+)^{42}\text{Sc}$	$2.70 \pm 0.74$	0.72	$3.75 \pm 1.09^d)$	$^{42}\text{Ca}(\text{p,n})^{42}\text{Sc}$	$3.24^e)$

a) results from refs /6-8,13/.

b) ref /9/.

c) ref /14/. d) 10% uncertainty is assumed for the "calculated fraction" in determining this number.

e) ref /15/.

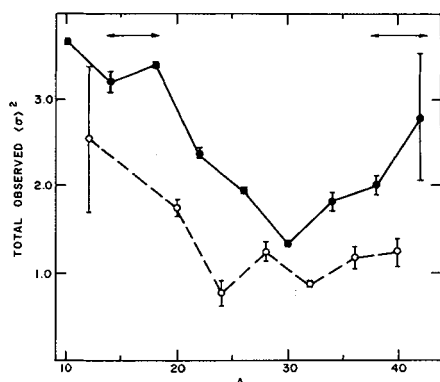


Fig. 5 Total observed  $\langle\sigma\rangle^2$  for the decay of all measured  $\beta^+$ -decays of  $T_Z = -1$  nuclei. Results for even-even nuclei appear as solid circles; those for odd-odd nuclei, as open circles. Results are from refs. /6-8,13/.

which prevail away from closed shells and lead to a more diffuse strength distribution (cf Fig. 3) with a smaller fraction lying within the  $\beta$ -decay window. The same general considerations can explain the consistently lower values seen for the decays of odd-odd nuclei compared with the  $0^+$  even-even parents, which populate only  $1^+$  states in their daughters.

Finally, if we focus on the four even-even decays that should nearly obey the limiting sum rule we can derive a measure of the missing strength. Our calculations for masses 14 and 18 confirm that the sum rule  $T_{\beta^+} \approx 6.0$  holds even with 10-20% 2-particle 2-hole admixtures in the parent ground state, so such a determination of the missing strength can be considered at least partially model independent. The results are summarized in Table 2. The average fraction of the sum rule exhausted is  $0.61 \pm 0.04$ , a result that agrees reasonably well with level-by-level shell model comparisons in the same mass region /17,18/, but is somewhat higher than that obtained from (p,n) data /19/.

With this result we can return to the decay of  $^{33}\text{Ar}$ . If it is assumed that the total reduction in strength to be observed in  $^{33}\text{Ar}$  is the same as that observed for

Table 2: Fraction of sum rule exhausted in four selected nuclear decays

$\beta^+$ -decay	Corrected $T_{\beta^+}$	$T_{\beta^+}/6$
$^{14}\text{O}(\beta^+)^{14}\text{N}$	$3.80 \pm 0.16$	$0.63 \pm 0.04$
$^{18}\text{Ne}(\beta^+)^{18}\text{F}$	$3.90 \pm 0.24$	$0.65 \pm 0.04$
$^{38}\text{Ca}(\beta^+)^{38}\text{K}$	$2.98 \pm 0.35$	$0.50 \pm 0.06$
$^{42}\text{Ti}(\beta^+)^{42}\text{Sc}$	$3.75 \pm 1.09$	$0.63 \pm 0.18$

the  $T_Z = -1$  nuclei just discussed, then the total Gamow-Teller strength likely to be available to  $^{33}\text{Ar}(\beta^+)^{33}\text{Cl}$  is  $\approx 5.8$  ( $=0.64 \times 9$ , ignoring energy limitations). The total strength shown in Fig. 2 is about 30% of that available and therefore does not represent a complete picture of the Gamow-Teller giant resonance. While it is possible that the observed energy range can be extended with more detailed experiments, it seems unlikely that a majority of the strength in fact lies within the energy-allowed decay window.

### III - $\beta$ -Decay of Heavy Nuclei

All heavier nuclei, even the most exotic, are characterized by  $N > Z$ . Consequently, as illustrated in Fig. 1, the main Gamow-Teller resonance is precluded from view in  $\beta^+$  and  $\beta^-$  decays; only its tail will contribute to the observed transitions. It is possible, nevertheless, to examine the anatomy of this tail in some detail in decays chosen to combine large  $Q$ -values with a high density of daughter states. Such decays are found in a wide variety of exotic nuclei.

Under such conditions it is no longer useful to consider the Gamow-Teller strength  $\langle \sigma \rangle^2$  for an individual transition. Instead we shall use the strength function  $S_\beta = \sum_i \langle \sigma \rangle_i^2 / \Delta E$ , which is the Gamow-Teller strength per energy interval. Thus, in analogy with eqn (2), the total decay rate to states in an energy interval  $\Delta E$  at excitation  $E_x$  is given by:

$$\sum \lambda_i / \Delta E = f S_\beta(E_x) (1.792 \pm 0.022) \times 10^{-4} \text{ s}^{-1} \quad (5)$$

Evidently the sum rule of eqn (4) still applies, with  $T_\beta$  now defined as

$$T_\beta = \int S_\beta(E_x) dE_x \quad (6)$$

Before discussing the results from heavy nuclei, it is necessary to describe some experimental limitations. The most common method of investigating a  $\beta$ -decay scheme is to measure the spectrum of  $\beta$ -delayed  $\gamma$ -rays with a high-resolution Ge spectrometer, and reconstruct the decay scheme, transition by transition, relying upon the observed relative intensities of  $\gamma$ -rays. While superficially straightforward, if tedious, this method has been shown /20/ to suffer severe limitations in the measurement of  $S_\beta$ . A fictional, but statistically realistic, nucleus called pandemonium was used to demonstrate that considerable  $\beta$ -decay strength is missed through the very large number of weak unobserved  $\gamma$ -ray peaks that must occur as a direct result of Porter-Thomas statistics. A careful study of the decay of  $^{145}\text{Gd}$  supports this conclusion /21/ despite one claim to the contrary /22/.

The inherent difficulty of discrete-line  $\gamma$ -ray spectroscopy in the extraction of  $\beta$ -strength functions can be overcome through the use of a "total absorption" spectrometer /23,24/, in which two NaI(Tl) detectors observe with very high efficiency the total  $\gamma$ -ray energy emitted in coincidence with each  $\beta$ -particle. Although the  $\gamma$ -ray resolution is low, a direct correlation can be made between the energy (and intensity) observed and that of the preceding  $\beta$ -transition, without recourse to any knowledge of the detailed decay scheme. Examples of results for  $\beta^+(\text{ec})$ -decay /23/ and  $\beta^-$ -decay /24/ appear in Figs. 6 and 7 respectively.

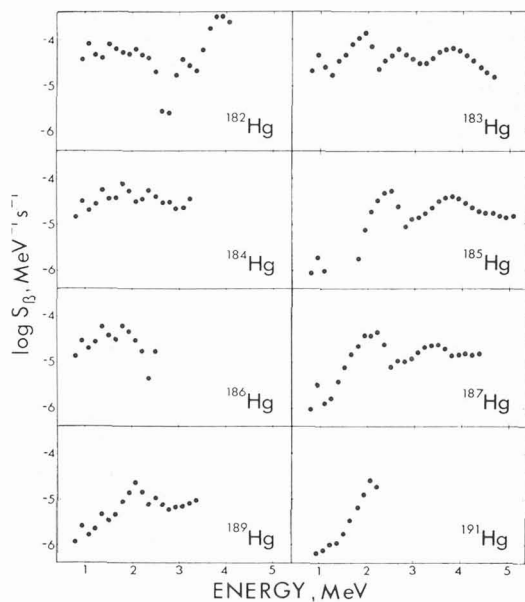


**Fig. 6** Beta strength functions measured /23/ for neutron-deficient isotopes of mercury, plotted as a function of excitation energy in the daughter. The ordinate of this figure, which is reproduced directly from ref /23/, must be multiplied by 3868 to yield  $S_\beta$  as defined in eqn (5).

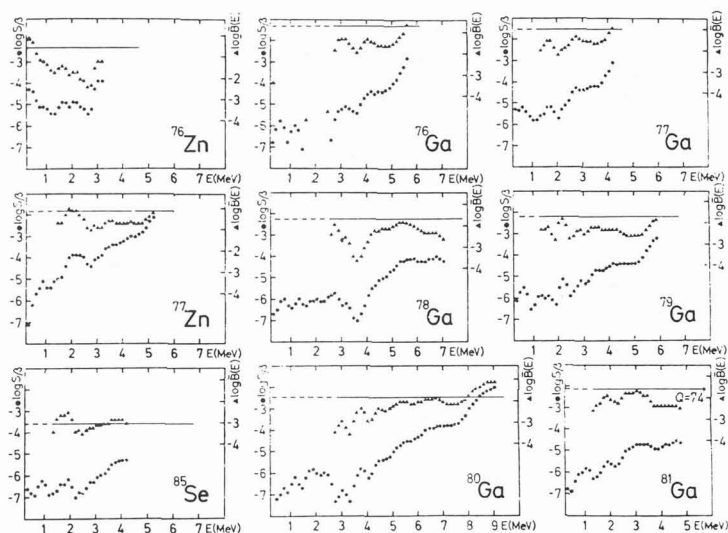


**Fig. 7** Beta strength functions measured /24/ for neutron-rich isotopes of zinc, gallium and selenium. The ordinate of this figure, which is reproduced directly from ref /24/, must be multiplied by 3868 to yield  $S_\beta$  as defined in eqn (5). The triangles give the average decay rate per transition, i.e.  $S_\beta$  divided by the level density. The abscissa is excitation energy in the daughter.



An interesting approach to collecting these data on  $\beta$ -strength functions has been presented recently by Behr and Vogel /25/. They considered two bodies of data: one based on high-resolution  $\gamma$ -ray studies of 107 fission fragments (the Evaluated Nuclear Data File); the other, the total-absorption low-resolution  $\gamma$ -ray measurements on 62 nuclei, taken from ref /24/, which was also the source of Fig. 7. The results appear in Figs. 8 and 9, respectively, where they have been combined according to their  $Q_\beta$ -value. For example, the series of joined dots labeled 7.5 constitutes the averaged strength for all decays with  $7.0 \leq Q_\beta \leq 8.0$ , plotted as a function of  $\beta$ -energy.

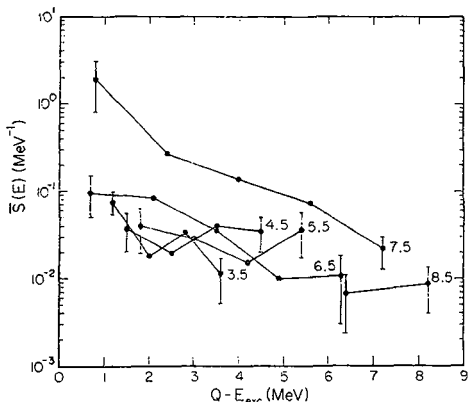
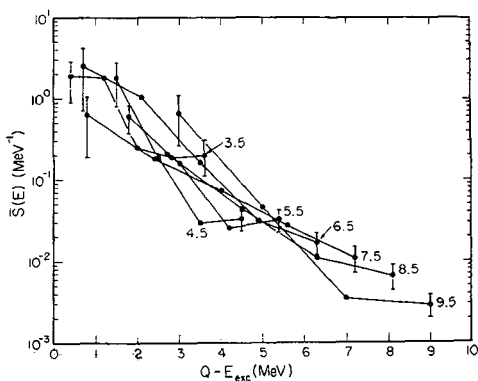


**Fig. 8** Average  $\beta$ -strength function for 107 neutron-rich nuclei with  $72 \leq A \leq 154$ . Data are collected according to total  $Q_\beta$  (e.g.  $7 \leq Q_\beta \leq 8$  is labeled 7.5) and plotted against  $\beta$  energy. The ordinate of this figure, which is reproduced directly from ref /25/, must be multiplied by 0.62 to yield  $S_\beta$  as defined in eqn (5).

Two significant conclusions can be drawn from Figs. 8 and 9. The first is that they further confirm the "pandemonium" conclusions: the strength functions of Fig. 8 are consistently lower than those of Fig. 9, with the biggest discrepancies being at lowest decay energies; evidently, strength is indeed consistently missed when discrete  $\gamma$ -ray spectra are used for extracting  $\beta$ -strength functions. The second is that a reasonably consistent picture is obtained (in Fig. 9) of average  $\beta$ -strength

**Fig. 9** Average  $\beta$ -strength function for 62 neutron-rich nuclei with  $76 \leq A \leq 145$ .



functions in the energy region available. To put that region in perspective, however, we should note that on the abscissa of Figs. 8 and 9 the analogue state in these nuclei would lie below -10 MeV, with the centre of the Gamow-Teller resonance still further away. Consistent with that observation is the fact that the maximum values observed for  $S_\beta$  are  $\approx 1 \text{ MeV}^{-1}$ , whereas the sum rule,  $3(N-Z)$ , for these nuclei lies between 36 and 100.

Another view of the strength function in exotic nuclei is provided by  $\beta$ -delayed particle emission, the process in which  $\beta$ -decay populates daughter states that are unstable to particle emission. Because particle emission usually leads to states at low excitation, the particle spectrum is frequently simple with a direct correlation between the particle spectrum shape and the strength function of the preceding  $\beta$ -decay. Both delayed-proton and delayed-neutron spectra have been used for this purpose. Their advantage over  $\gamma$ -ray studies is that detector efficiencies and response functions, particularly for protons, are better known; but they have the disadvantage that several factors other than the  $\beta$ -decay influence the spectrum strongly.

The general scheme for delayed-proton decay appears in Fig. 10. The average intensity of protons with energy  $E_p$  is given by /26/

$$I_p(E_p) = \sum_{if} \langle I_{\beta}^i \rangle_{E_p} \frac{\Gamma_p^{if}}{\Gamma_p^i + \Gamma_Y^i} \quad (7)$$

where  $I_{\beta}^i$  is the intensity of  $\beta$ -decay from the precursor to excited state  $i$  in the emitter,  $\Gamma_p^{if}$  is the partial width for proton emission between state  $i$  and final state  $f$  in the daughter,  $\Gamma_p^i$  is the total proton decay width of state  $i$ , and  $\Gamma_Y^i$  is the  $\gamma$ -decay width. Here  $\langle \rangle$  denotes the (Porter-Thomas) statistical mean, and the summation is extended over all pairs of states  $i$  and  $f$  between which protons of energy  $E_p$  can be emitted. Following eqn (2) we write

$$\langle I_{\beta}^i \rangle_{E_p} = \langle f S_{\beta}(E_p^i) \rangle t_{1/2} (2.585 \pm 0.032) \times 10^{-4} \quad (8)$$

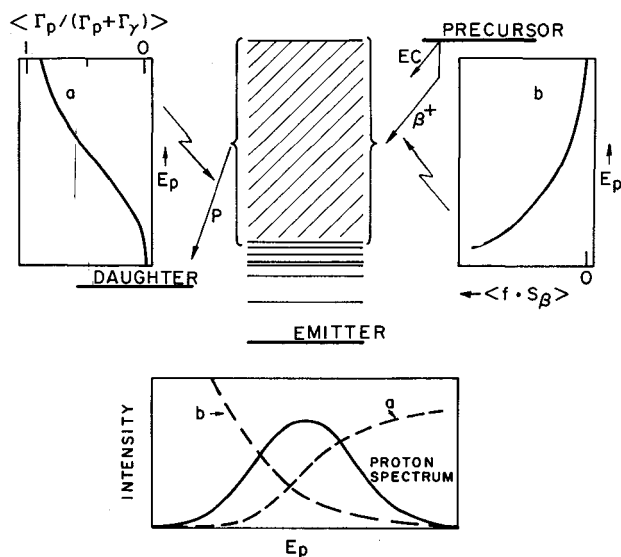


Fig. 10  
The upper central portion of the figure illustrates the general decay scheme of a delayed-proton precursor. The graphs labeled a and b at the upper left and right show the behaviour of  $\langle \Gamma_p / (\Gamma_p + \Gamma_Y) \rangle$  and  $\langle f S_{\beta} \rangle$ , respectively, as a function of proton energy. The graph at the bottom demonstrates how these two functions combine in determining the delayed proton spectrum.

Clearly, if the behaviour of  $S_{\beta}(E_p)$  is to be extracted from  $I_p(E_p)$ , an accurate knowledge of  $\Gamma_p$  and  $\Gamma_Y$  must first be obtained independently.

This has become possible through an experimental technique only feasible for exotic nuclei: the proton X-ray coincidence technique (PXCT) /27/. It involves the measurement of the ratio of daughter X-rays as a function of the energy of coincident delayed protons, and yields the average level widths,  $\Gamma \approx 1$  eV, of the proton

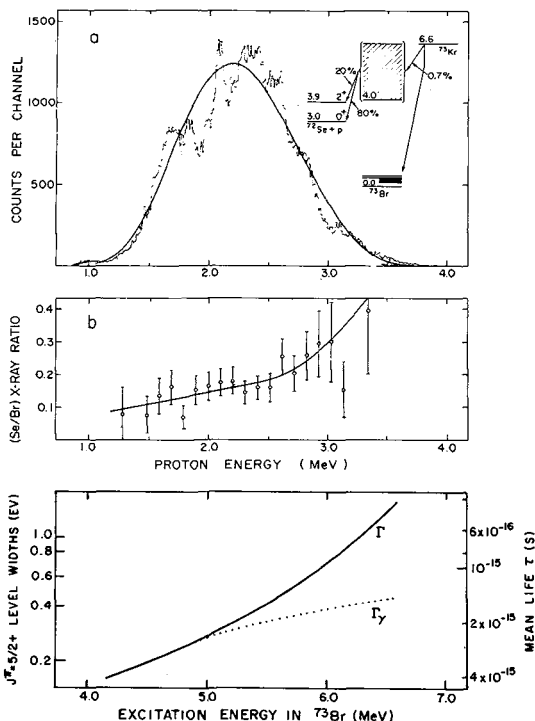
emitting states. Results for  $^{73}\text{Kr}$  decay appear in Fig. 11. Although the PXCT specifies  $\langle\Gamma_\gamma\rangle$  and  $\langle\Gamma_p\rangle$  rather well (see Fig. 11b,c) we are less secure in our knowledge of the individual  $\Gamma_{if}^p$  values of eqn (7). Here it is necessary to rely upon the optical model and the belief that an even-even daughter nucleus will exhibit approximately equal spectroscopic factors to its various states f. With these qualifications, however, we can consider that for a case like that of  $^{73}\text{Kr}$ , the right-hand factor in eqn (7) is determined, and the proton spectrum can be used as a measure of  $\langle\Gamma_\beta^i\rangle$  or, through eqn (8),  $S_\beta$ .

Fig. 11

a) Spectrum of protons observed following the decay of  $^{73}\text{Kr}$ . In the simplified decay scheme, which is inset, all energies are given in MeV relative to the  $^{73}\text{Br}$  ground state.

b) Ratio of X rays from Se relative to those from Br, plotted as a function of coincident proton energy

c) Level widths required for agreement with data in b. The same result is used to calculate the smooth curve in a.



It is convenient in delayed-proton analysis to adopt a model for  $S_\beta(E_\beta)$  and test its validity against the observed proton spectrum. The agreement shown in Fig. 11a between calculation and experiment demonstrates the success of this approach for  $^{73}\text{Kr}$  if the strength-function energy-dependence is adopted from the "gross-theory" of  $\beta$ -decay /28/. For the present purposes there is no need to describe the precepts of this theory; it is sufficient to show, in Fig. 12, the strength functions calculated with the theory for a series of  $T_Z = 1/2$  delayed-proton precursors including

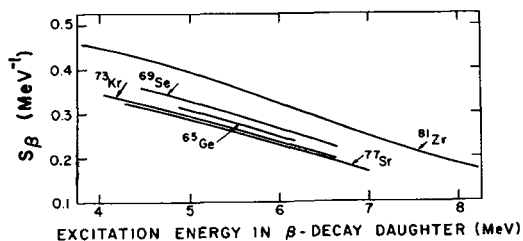


Fig. 12 Strength functions calculated according to the "gross theory" for the  $\beta$ -decay of  $T_Z = 1/2$  precursors.

$^{73}\text{Kr}$ . It can be seen in Fig. 13 that the quality of the agreement with experiment for  $^{73}\text{Kr}$  is indeed typical for all five. It should be noted that only the energy dependence of  $S_\beta$  is tested by the comparisons of Fig. 13. The absolute magnitude of  $S_\beta$  is reflected in the branching ratio (or partial half-life) for proton emission. We shall return to this aspect later.

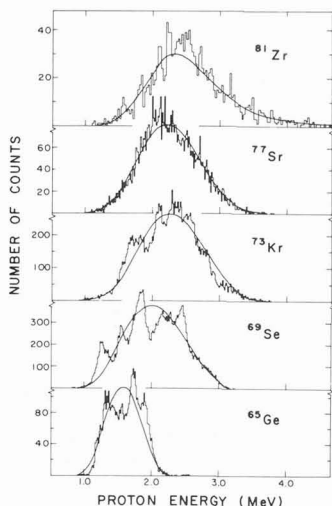


Fig. 13 Delayed proton spectra observed for precursors in the  $T_z = 1/2$  series. Curves are the results of calculations with the  $\beta$ -strength functions of Fig. 12. Details are given in ref /29/.

Not all delayed-proton precursors show such excellent agreement with the "gross theory" strength functions. Figure 14 gives the results for three xenon isotopes, illustrating the sensitivity of the spectra to changes in  $S_\beta$ , and demonstrating the need for rather steeply rising strength functions. Unfortunately, the limited energy range makes it impossible to conclude whether we are observing the rise to a local peak, or some major feature of the giant resonance.

Similar information is available from the study of  $\beta$ -delayed neutron emission. Delayed neutron spectra can be described by equations analogous to (7) and (8), which are somewhat simpler to calculate because the Coulomb barrier plays no role. However, neutron emission precludes use of the PXCT measurement for  $\Gamma$ , and this results in much greater uncertainty in extracting a reliable  $S_\beta$ . Nevertheless, strength functions have been extracted from experiment in a number of cases. An example is shown in Fig. 15 for a series of rubidium isotopes. Note that only results from the three heaviest isotopes incorporate delayed neutron data, but all use  $\beta$ -delayed  $\gamma$ -ray data obtained with high-resolution spectroscopy and presumably subject to the pandemonium deficiencies already described. Unlike the delayed proton results, these show several pronounced peaks, although all are in the region accessed by  $\gamma$ -ray measurements or are near  $Q_\beta$  where experimental uncertainties are greatest.

If we accept these features, for  $^{95}\text{Rb}$  for example, then shell-model calculations - whether with the RPA as shown in the figure or with the Brown-Bolsterli model /32/ used by Klapdor /33/ and recently discussed by Kratz /34/ - show better agreement with the experimental strength function than the "gross theory", which is simply based on a modified Fermi gas model. However, for  $^{97}\text{Rb}$  the same shell-model calculations fail completely to reproduce the featureless function indicated by experiment, at least below 9 MeV. In this case the "gross theory" does rather well, as is also confirmed by the comparison between the calculated and experimental neutron spectra shown for  $^{97}\text{Rb}$  in Fig. 16. The identification of prominent features and their consistent reproduction (or prediction) by calculation in such nuclei must still be regarded as an open question.

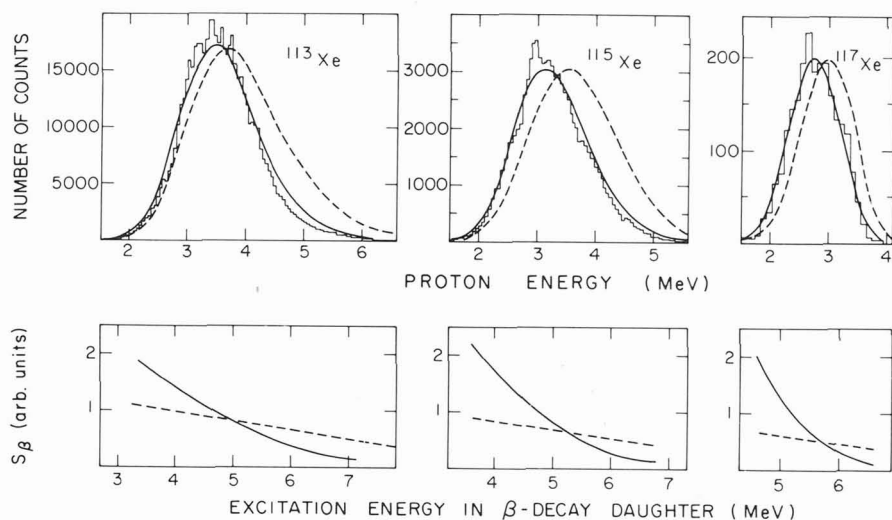


Fig. 14 (top) Delayed proton spectra observed for three xenon precursors. Curves are the results of calculations with the strength functions shown below. (bottom) Beta strength functions,  $S_\beta$ , used in calculating the delayed proton spectra shown above. The dashed curves were obtained from the "gross theory" of  $\beta$ -decay; the solid curves were derived empirically to produce improved agreement with the delayed-proton data.

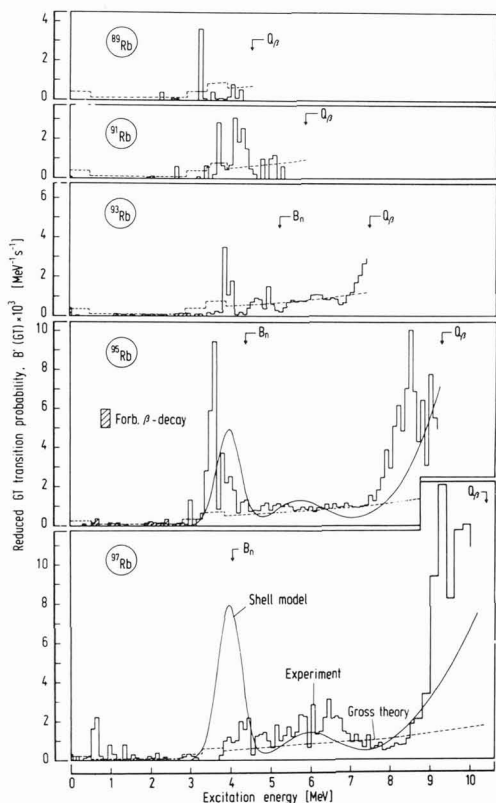
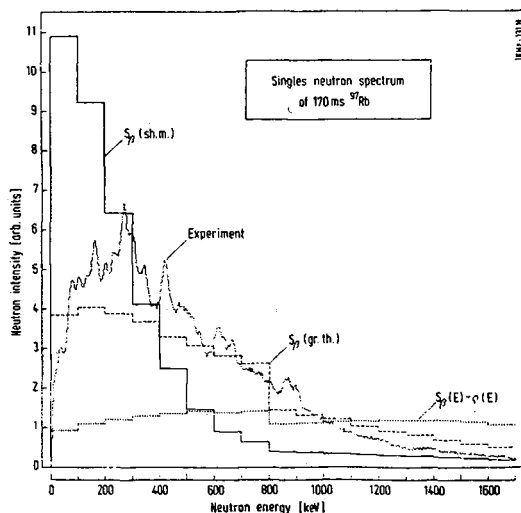


Fig. 15 Experimental  $\beta$ -strength functions of odd-mass rubidium isotopes plotted as a function of excitation energy in their daughters and taken from ref /30/. The quantity  $B'(GT)$  is essentially equivalent to  $S_\beta$  as defined in eqn (5). The  $Q_\beta$  and neutron separation energy,  $B_n$ , are noted. For comparison, calculated strength functions are shown from the "gross theory" /28/ and a shell-model RPA approach /31/.

So far in our discussion of delayed particle emitters, we have dealt only with strength-function shapes. In many cases, though, the precursor half-life and the branching ratio for proton (or neutron) emission is known. Thus the magnitude of  $S_\beta$  can be determined, as well as its energy dependence. For delayed-proton emitters this means, in effect, that functions such as those shown in Fig. 12 are scaled until agreement with the experimental branching ratio is achieved. For delayed-neutron emitters we have taken a different approach since neutron branching ratios ( $P_n$ ) are known for many cases where detailed strength functions have not been determined. From eqn (5) we can write

$$\bar{S}_\beta = (P_n/t_{1/2})(3867/\int_0^{Q_\beta - B_n} f dE) \quad (9)$$

where  $\bar{S}_\beta$  is the average strength function over the region of excitation where neutrons are emitted. This equation ignores competing X-ray emission and is therefore not exact, but it should give a reasonable result. Figure 17 shows a summary of delayed proton /29/ and delayed neutron /35/ data treated in this way. The delayed neutron data agree rather well with the data in Fig. 9 if the different normalizations are taken into account. They are for comparable neutron-rich nuclei and confirm that in such nuclei very little of the total Gamow-Teller strength  $T_\beta^-$  contributes to  $\beta^-$ -decay. By contrast, the delayed proton precursors,  $\beta^+$ -emitters with much smaller values of  $(N-Z)$ , yield much higher values of  $S_\beta$ . Likely this reflects a larger  $T_\beta^+$ , caused by the lower neutron excess, rather than a larger fraction of  $T_\beta^+$  contributing to the observed  $\beta^+$ -decay.



**Fig. 16**  
Comparison between the experimental singles neutron spectrum of  $^{97}\text{Rb}$  taken from ref /34/. In addition to shell model /31/ and "gross theory" /28/ calculations,  $S_\beta(E) \approx \rho(E)$  is also shown for comparison.

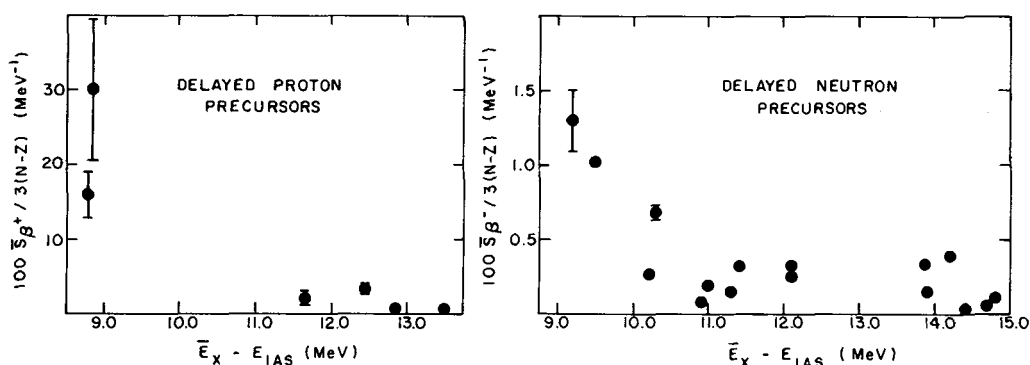


Fig. 17 Average strength functions measured from delayed proton and neutron precursors expressed as a fraction of the sum rule,  $3(N-Z)$ , and plotted as a function of excitation energy in the daughter relative to the isobaric analogue state. Results for  $^{109}\text{Te}$  ( $S_{\beta} = 253 \text{ MeV}^{-1}$ ) and  $^{73}\text{Kr}$  ( $S_{\beta} = 700 \text{ MeV}^{-1}$ ) have been omitted as apparent experimental errors. If they could be confirmed, they would be very interesting results.

#### IV - CONCLUSION

There is little doubt that the only region where  $\beta$ -decay samples a large fraction of the total distribution of Gamow-Teller strength is in the  $\beta^+$ -decay of neutron-deficient light nuclei. These cases confirm the conclusions drawn from (p,n) studies, in which significant strength is found missing. For heavier nuclei, only the tail of the Gamow-Teller resonance participates in  $\beta^+$ -decay as is indicated by the weakness of the observed strength function. Its shape is also consistent with this conclusion although features from local nuclear structure are likely superimposed.

#### REFERENCES

1. KOSLOWSKY V.T. *et al*, Contribution to International Conference on Nuclear Physics, Florence, Italy (1983).
2. WILKINSON D.H., Nucl. Phys. **A377** (1982) 474.
3. NAKAYAMA K. *et al*, Phys. Lett. **114B** (1982) 217.
4. HARDY J.C. *et al*, Phys. Rev. **C3** (1971) 700.
5. GAARDE C. *et al*, Nucl. Phys. **A334** (1980) 248.
6. AJZENBERG-SELOVE F., Nucl. Phys. **A360** (1981) 1.
7. WILSON H. *et al*, Phys. Rev. **C22** (1980) 1696.
8. HERNANDEZ A.M. and DAHNICK W., Phys. Rev. **C24** (1981) 2235.
9. GOODMAN C., Nucl. Phys. **A374** (1982) 241.
10. FRENCH J.B. *et al*, in Adv. In Nucl. Phys. vol. 3, ed. E. Vogt & M. Baranger (Plenum, N.Y., 1969).
11. COHEN S. and KURATH D., Nucl. Phys. **73** (1965) 1.
12. FREEDOM B.M. and WILDENTHAL B.H., Phys. Rev. **C6** (1972) 1633.
13. ENDT P.M. and VAN DER LEUN C., Nucl. Phys. **A310** (1978) 1.
14. ANDERSON B.D. *et al*, Phys. Rev. **C27** (1983) 1387.
15. GOODMAN C.D. *et al*, Phys. Lett. **107B** (1981) 406.
16. GAARDE C. *et al*, Nucl. Phys. **A369** (1981) 258.
17. WILKINSON D.H., Nucl. Phys. **A209** (1973) 470.
18. BROWN B.A. *et al*, Phys. Rev. Lett. **40** (1978) 1631.
19. GAARDE C. Nucl. Phys. **A396** (1983) 127.
20. HARDY J.C. *et al*, Phys. Lett. **71B** (1977) 307.
21. HARDY J.C. *et al*, Phys. Lett. to be published.

22. FIRESTONE R.B., Phys. Lett. 113B (1982) 129.
23. HORNSHØJ P., et al, Nucl. Phys. A239 (1975) 15.
24. ALEKLETT K., et al, Nucl. Phys. A246 (1975) 425.
25. BEHR J.R. and VOGEL P., to be published.
26. MACDONALD J.A. et al, Nucl. Phys. A288 (1977) 1.
27. HARDY J.C. et al, Phys. Rev. Lett. 37 (1976) 133.
28. TAKAHASHI K. et al, Atomic and Nucl. Data Tables 12 (1973) 101.
29. HARDY J.C., Proc. Int. Conf. Nuclei far from Stability, 4th, Helsingor, 1981  
CERN rep 81-09 pg. 217.
30. KRATZ K-L, et al, Z. Physik A312 (1983) 43.
31. OLIVEIRA Z.M. de, PhD thesis, Univ. of California, Berkeley (1980).
32. BROWN G.E. and BOLSTERLI M., Phys. Rev. Lett. 3 (1959) 472.
33. KLAPDOR H.V. et al, Z. Physik A299 (1981) 213.
34. KRATZ K-L, Nucl. Phys. to be published.
35. HOFF P., Proc. Int. Workshop on Gross Properties of Nuclei and Nuclear  
Excitations VII, Hirschegg, Austria (1979): INKA-Conf-79-001-058.